1 **Title:** The common *TMEM173 HAQ, AQ* alleles rescue CD4 T cell death, restore T-regs, and
2 prevent *SAVI (N153S)* inflammatory disease in mice

3 **Authors/Affiliations:** Alexandra Aybar-Torres[1], Lennon A Saldarriaga[1], Ann T. Pham[1], Amir
4 M. Emtiazjoo[1], Ashish K Sharma[2], Andrew J. Bryant[1] and Lei Jin[1*]

5 [1]Division of Pulmonary, Critical Care and Sleep Medicine, Department of Medicine,

6 [2]Division of Vascular Surgery & Endovascular Therapy, Department of Surgery, University of
7 Florida, Gainesville, FL 32610, U.S.A

8

9 ***Corresponding Author:**

10 Lei Jin, Ph.D.

11 1600 SW Archer Road, P.O.Box 100225, Gainesville, FL, 32610

12 Fax : 352-273-9154

13 Phone: 352-294-8495

14 Email: lei.jin@medicine.ufl.edu

15

Abstract

STING activation induces lymphocyte cell death that is independent of type I IFNs. The *in vivo* significance and mechanism of STING-mediated cell death is unclear. Using STING knock-in mice, we found that lymphocytes from the *HAQ*, *AQ*, and *Q293* mice are resistant to STING-mediated cell death *ex vivo*, establishing a critical role of STING residue 293 in cell death. CD4 T cellpenia is evident in STING-associated vasculopathy with onset in infancy (SAVI), an autosomal dominant, fatal inflammatory disease caused by gain-of-function human STING mutations. The *HAQ/SAVI(N153S)* and *AQ/SAVI(N153S)* mice have similar spleen CD4 T cells as the *WT* mice reversing the CD4 T cellpenia by the gain-of-function N153S STING. The *HAQ/SAVI(N153S), AQ/SAVI(N153S)* mice have more (~10-fold, ~20-fold, respectively) T-regs than *WT/SAVI(N153S)* mice. Remarkably, while have comparable TBK1, IRF3, NFκB activation as the *WT/SAVI*, the *AQ/SAVI* mice have no tissue inflammation, regular body weight, and normal lifespan. The type I IFNs-independent function of STING in health and diseases has been increasingly recognized. We propose that STING activation promotes tissue inflammation by depleting T-regs cells *in vivo*. Billions of modern humans have the dominant *HAQ, AQ* alleles. STING research and STING-targeting immunotherapy should consider *TMEM173* heterogeneity in humans.

Keywords: STING, *HAQ AQ TMEM173* alleles, tissue inflammation, SAVI, T-regs

One-sentence summary: The Common *TMEM173* alleles *HAQ, AQ* prevent SAVI disease.

Introduction

STING drives cytosolic DNA-induced type I IFNs production [1]. Recent research revealed that STING promotes inflammation in a variety of inflammatory diseases including nonalcoholic fatty liver disease, nonalcoholic steatohepatitis, kidney injury, neurodegenerative diseases, cardiovascular diseases, obesity, diabetes, and aging [2-9]. The type I IFNs-independent function of STING has also emerged [10,11]. For example, initially described as a type I interferonopathy [12], the symptoms of STING-associated vasculopathy with onset in infancy (SAVI) are largely independent of type I IFNs [13-16]. In a STING N153S mouse model of SAVI, crossing N153S mice to cGAS, IRF3/IRF7, and IFNAR1 knockout mice, N153S mice still developed spontaneous lung diseases [13]. In another example of STING-dependent, type I IFNs-independent inflammatory disease, DNase II-deficient mice developed autoinflammatory arthritis that can be rescued by STING deficiency [17]. But *Dnase II*$^{-/-}$ mice with the STING-S365A mutation still exhibited severe polyarthritis [18,19]. The STING-S365A mutant cannot recruit IRF3 and produce IFNβ [10,11,18,19]. How STING drives inflammation *in vivo,* independent of type I IFNs, remains unknown. The activation of NFκB or NLRP3 inflammasome by STING has been proposed [9,20].

Characterized as an innate immune sensor, STING expression is, paradoxically, high in CD4 T cells [12,21]. Furthermore, STING activation kills mouse and human CD4 T cells *ex vivo* [22-24]. SAVI patients and mouse model had CD4 T cellpenia [12,24]. STING was first discovered as MPYS for its cell growth inhibition and cell death function in mouse B lymphoma cells [25]. STING-mediated cell death is cell type dependent. For example, while STING activation kills human endothelial cells, primary and cancerous T cells, it does not kill mouse MEFs, BMDCs, or BMDMs [26-28]. Second, STING-mediated cell death is type I IFNs-independent [24,26,28]. Multiple cell death pathways, i.e., apoptosis, necroptosis, pyroptosis, ferroptosis, and PANoptosis, are triggered [28-30]. Last, the *in vivo* biological significance of STING-mediated CD4 T cell death is not clear [24,28]. WT and STING$^{-/-}$ mice have similar thymic and pLN CD4^{-}CD8^{-}, CD4^{+}CD8^{+}, and single positive CD4 and CD8 T cell populations [22,23]. The expression of CD4 and CD8 TCR are comparable [22,23]. The naive, memory, or regulatory T cell populations are similar in WT and STING$^{-/-}$ mice that expressed comparable levels of CD69 and CD25 following TCR activation [22,23]. Together, the absence of STING in mice does not alter T cell development or TCR signaling [22]. In humans, SAVI patients with constitutively activated STING have low CD4 T cell numbers [12], and type I

67 IFNs are dispensable for STING-mediated human CD4 T cell death [24]. Notably, SAVI patients
68 (N154S or V155M) had similar counts of CD8 T and B cells [12].

69 Also, unlike other innate immune genes, the human *TMEM173* gene is highly heterogeneous
70 [31,32]. ~50% of people in the U.S. carry at least one copy of non-*WT (R232) TMEM173* allele [31].
71 Among them, the R71H-G230A-R293Q (*HAQ*) is the 2nd most common *TMEM173* allele carried
72 by ~23% of people in the U.S. [31]. However, in East Asians, *WT/HAQ* (34.3%), not *WT/WT*
73 (22.0%), is the most common *TMEM173* genotype [32]. Critically, the *HAQ* allele was positively
74 selected in modern humans outside Africa [33]. Anatomically modern humans outside Africa are
75 descendants of a single Out-of-Africa Migration 50,000~70,000 years ago. ~1.4% of Africans have
76 the *HAQ* allele, while ~63.9% of East Asians are *HAQ* carriers [33]. Haplotype analysis revealed that
77 *HAQ* was derived from G230A-R293Q (*AQ*) allele [33]. Importantly, the *AQ* allele was negatively
78 selected outside Africa [33]. ~40.1% of Africans are *AQ* carriers, while ~0.4% of East Asians have
79 the *AQ* allele [33]. Importantly, *TMEM173* alleles often have a dominant negative effect because the
80 protein product STING exists as a homodimer [25,34]. For example, SAVI is an autosomal dominant
81 inflammatory disease [35]. *WT/HAQ* individuals had reduced Pneumovax23®-induced antibody
82 responses compared to *WT/WT* individuals (NCT02471014) [36]. Notably, *AQ* responds to CDNs
83 and produce type I IFNs *in vivo* and *in vitro* [33,37,38], but the *AQ* allele was negatively selected in
84 non-Africans [33]. In contrast, the *HAQ* allele, defective in CDNs-type I IFNs responses [31,32,36,39,40],
85 was positively selected in non-Africans[33] indicating that the CDNs-type I IFNs independent
86 function of STING was essential for the survival of early modern humans outside of Africa.

87 In this study, we discovered, surprisingly, that the *HAQ*, *AQ* cells are resistant to STING-
88 mediated lymphocyte death. We generated *HAQ/SAVI(N153S)* and *AQ/SAVI(N153S)* mice and
89 found that the *HAQ, AQ* alleles prevent CD4 T cellpenia, increase/restore T-regs and alleviate/stop
90 tissue inflammation in SAVI mice, thus providing evidence for the *in vivo* significance of type I
91 IFNs-independent, STING-mediated CD4 T cell death.

Results

STING activation kills mouse spleen CD4, CD8 T and CD19 B cells *ex vivo*.

We first used the synthesized non-CDNs STING agonist diABZI [41] to induce lymphocyte death because diABZI induces cell death [27,42] and diABZI is in clinical trials (NCT05514717). Splenocytes from C57BL/6N mice were treated with diABZI in culture, and cell death was determined by Annexin V and Propidium Iodide stain. Splenocyte cell death could be detected as early as 5hrs post diABZI treatment (Figure S1A), indicating that diABZI likely directly kills splenocytes rather than via the secondary cytokines, *e.g.* TNF, type I IFNs, et.al. Dosage responses showed that ~25ng/ml diABZI could kill 70% of splenocytes (Figure S1B). Similarly, STING agonists 2'3'-cGAMP, DMXAA, and synthetic CDNs RpRpssCDA, killed mouse spleen CD4, CD8 T cells, and CD19 B cells (Figure 1A). Thus, STING activation induces mouse lymphocyte death *ex vivo*.

TBK1 activation is required for STING-mediated mouse spleen cell death *ex vivo*.

STING activation can lead to apoptosis, pyroptosis, necroptosis, or ferroptosis [24-30,42,43]. We then treated mouse splenocytes with apoptosis, pyroptosis, necroptosis inhibitors, STING inhibitors H151, C176, palmitoylation inhibitor 2-bromopalmitate (2-BP), followed by diABZI stimulation. Inhibitors for NLRP3 (MCC950), RIPK1 (Necrostatin-1), RIPK3 (GSK872), Caspase-1 (VX-795), Caspase-3 (Z-DEVD-FMK), Caspase 1,3,8,9 (Q-VD-Oph), ferroptosis (liproxstatin-1) did not affect diABZI-induced splenocyte cell death *ex vivo* (Figure S1C, 1B). The STING inhibitors H151, C175, and 2-BP also could not prevent diABZI-induced cell death (Figure S1C). Instead, the TBK1 inhibitor Bx-795 treatment abolished diABZI-induced splenocyte death (Figure S1A).

BX-795 is a multi-kinase inhibitor including 3-phosphoinositide-dependent protein kinase 1 (PDK1) and TBK1 (IC_{50s} = 6 and 11 nM, respectively). However, the treatment of PDK1 inhibitor GSK2334470 (IC50 = 10nM) did not prevent diABZI-induced splenocyte death (Figure 1B). In contrast, GSK8612, a highly potent and selective inhibitor for TBK1, prevented diABZI-induced splenocyte death (Figure 1B). Thus, TBK1 activation is likely critical for STING-mediated lymphocyte cell death in mice.

HAQ, AQ, Q293 STING knock-in mouse splenocytes are resistant to STING-mediated cell death *ex vivo*.

123 *HAQ* and *AQ* are common human *TMEM173* alleles [31-33]. Previously, we reported that *HAQ* knock-
124 in mice are defective in CDNs-induced immune responses, while CDNs responses in *AQ* knock-
125 in mice are similar to WT mice [33]. We treated splenocytes from *HAQ* and *AQ* mice with diABZI
126 *ex vivo* and found, surprisingly, that both *HAQ* and *AQ* splenocytes were resistant to diABZI-
127 induced cell death (Figure 1C, 1D). In comparison, IFNAR1$^{-/-}$ splenocytes were killed by diABZI,
128 confirming that STING-mediated lymphocytes death are type I IFNs-independent (Figure 1C, 1D)
129 [24,26,28].

130 *HAQ* and *AQ* share the common A230 and Q293 residues changes. We thus generated a *Q293*
131 *TMEM173* knock-in mouse. Notably, the Q293 splenocytes were resistant to STING agonists 2'3'-
132 cGAMP, RpRpssCDA, and diABZI-induced cell death (Figure 1E, 1F). Thus, the residue 293 of
133 STING is critical for its cell death function.

134

135 ***WT/HAQ*, *WT/AQ* mouse splenocytes are partially resistant to STING-mediated cell death**
136 ***ex vivo*.**

137 *WT/HAQ* (34.3%), not *WT/WT* (22.0%), is the most common human *STING* genotype in East
138 Asians, while *WT/AQ* (28.2%) is the 2nd most common *STING* genotype in Africans [32]. We
139 generated *WT/HAQ*, *WT/AQ* mice and treated the splenocytes with mouse STING agonist
140 DMXAA. *WT/HAQ* and *WT/AQ* splenocytes were protected from 25µg/ml DMXAA-induced cell
141 death (Figure 1G). 100µg/ml DMXAA could kill *WT/HAQ* and *WT/AQ* splenocytes albeit less than
142 *WT/WT* cells (Figure 1G). Thus, the *HAQ* and *AQ* alleles are not recessive and likely impact
143 STING activation even in heterozygosity.

144

145 **STING activation kills primary human CD4 T cells, but not CD8 T or CD19 B cells**

146 STING agonists-based clinical trials in humans have been disappointing (NCT02675439,
147 NCT03010176, NCT05514717) [44,45]. We also showed that the human *TMEM173* gene might
148 undergo natural selection during the out-of-Africa migration [33] sensitive to evolutionary pressure.
149 Thus, we investigated STING-mediated death in primary human lymphocytes.

150 Human explant lung cells from the *WT(R232)/WT(R232)* donors were treated with STING
151 agonists 2'3-c GAMP, RpRpssCDA, diABZI for 24hrs in culture. Lymphocyte cell death was
152 determined by Propidium Iodide staining. Different from mouse lymphocytes, diABZI and

153 RpRpssCDA killed human CD4 T but not CD8 T or CD19 B cells (Figure 2A, 2B). Human CD8
154 T and CD19 B cells are resistant to 500ng/ml diABZI-induced cell death (Figure S2A).
155
156 ***WT/HAQ* human CD4 T cells are resistant to low-dose of diABZI-induced cell death.**
157 *WT/HAQ* mouse splenocytes are resistant to low dose diABZI-induced cell death. We obtained
158 lung explants from *WT/WT* and *WT/HAQ* individuals (Figure S2B) and treated them with diABZI
159 in culture. 25ng/ml diABZI killed *WT/WT*, but not *WT/HAQ*, lung CD4 T cells (Figure 2C).
160
161 **diABZI induces cell death in STING-KO human THP-1 cells reconstituted with *WT* human**
162 ***STING (R232)* but not *HAQ, AQ or Q293* human *STING* allele.**
163 To further determine cell death influenced by human *TMEM173* alleles *HAQ, AQ* and Q293, we
164 used the *STING-KO* THP-1 cell line because STING agonist induces type I IFNs and cell death in
165 *STING-KO* THP-1 cells expressing WT human STING [30] (Figure S2C, S2D). We, thus, generated
166 stable THP-1 *STING-KO* lines expressing *HAQ, AQ, WT* or *Q293 TMEM173* allele. Cell death
167 was determined by Annexin-V staining. diABZI killed THP-1 *STING-KO* lines expressing *WT* but
168 not *HAQ, AQ,* or *Q293 TMEM173* allele (Figure 2D, 2E). No cell death was induced in the *Q293*
169 THP-1 cells stimulated by 20 to 200 ng/ml of diABZI (Figure 2F). diABZI also did not induce
170 STING activatin in *Q293* THP-1 cells (Figure 2G). Notably, 50ng/ml diABZI induced p-IRF3
171 activation and type I IFNs in *AQ* THP-1 cells, but not *HAQ* THP-1 cells (Figure 2H, 2I, 2J)
172 indicating that the STING-cell death and STING-IRF3-Type I IFNs pathways can be uncoupled.
173
174 ***HAQ* and *AQ* alleles rescue the lymphopenia and suppress myeloid cell expansion in**
175 ***SAVI(N153S)* mice.**
176 The *in vivo* significance of the STING/MPYS-cell death is unclear. SAVI is an autosomal
177 dominant, inflammatory disease caused by gain-of-function STING mutation [12]. CD4 T cellpenia
178 was found in SAVI patients and SAVI mouse models [12,13]. We thus generated *HAQ/SAVI(N153S)*
179 and *AQ/SAVI(N153S)* mice aiming to restore CD4 T cells in SAVI mice to establish the *in vivo*
180 significance of STING/MPYS-cell death.
181 First, *HAQ/SAVI(N153S)* and *AQ/SAVI(N153S)* mice had reduced splenomegaly compared to
182 *WT/SAVI(N153S)* mice though their spleens were still larger than the littermates *WT/HAQ* and
183 *WT/AQ* (Figure 3A, 3B). Next, *HAQ/SAVI(N153S)* and *AQ/SAVI(N153S)* mice had similar spleen

184 B cells and CD4 T cells numbers as the *WT/HAQ*, *WT/AQ* mice (Figure 2B, 2C). Their $CD8^+$ T
185 cells were lower than their WT littermates but much higher than the *WT/SAVI(N153S)* mice (Figure
186 3D). Third, spleen myeloid cell numbers, i.e., neutrophils, $Ly6C^{hi}$ monocytes and F4/80
187 macrophages, were all reduced by half compared to *WT/SAVI(N153S)* mice (Figure 3E~3H).
188 Notably, the *HAQ/SAVI(N153S)* and *AQ/SAVI(N153S)* mice also had restored bone marrow
189 monocyte (Figure S3). Thus, *HAQ* and *AQ* alleles prevent lymphopenia and suppress myeloid cells
190 expansion in *SAVI(N153S)* mice.
191
192 **The *HAQ* allele alleviates and the *AQ* allele prevents *SAVI(N153S)* disease in mice**.
193 *SAVI(N153S)* disease is characterized by early onset, failure to thrive (low body weight), persistent
194 lung inflammation, decreased lung function, and young death in humans and mouse models
195 [12,16,46,47]. The *HAQ/SAVI(N153S)* mice weighed more and had an improved lifespan than the
196 *WT/SAVI(N153S)* mice (Figure 4A, 4B). The lifespan, airway resistance and tissue inflammation
197 were also improved in *HAQ/SAVI(N153S)* mice compared to the *WT/SAVI(N153S)* mice (Figure
198 4C, 4D, 4J, 4K, S4). However, the pulmonary artery pressure was still elevated in
199 *HAQ/SAVI(N153S)* mice (Figure 4E). Remarkably, the *AQ/SAVI(N153S)* mice had similar body
200 weight and lifespan as the *WT/AQ* mice (Figure 4F, 4G). The airway resistance, pulmonary artery
201 pressure, and tissue inflammation in *AQ/SAVI(N153S)* were similar to the *WT/AQ* mice (Figure
202 4H, 4I, 4J, 4K, S4). Thus, the *AQ* allele prevents inflammatory SAVI disease in mice.
203
204 **diABZI induces similar STING, TBK1, IRF3, NFκB activation in the *AQ/SAVI(N153S)* and**
205 ***WT/SAVI(N153S)* BMDM.**
206 SAVI was characterized as type I interferonopathy [16]. However, several studies showed that type
207 I IFN signaling and IRF3 activation were dispensable for SAVI disease [13,14,47,48]. *AQ* allele prevents
208 SAVI disease (Figure 4). However, diABZI-treated *AQ/SAVI(N153S)* and *WT/SAVI(N153S)*
209 BMDM had similar TBK1-IRF3 activation (Figure 5A). Furthermore, diABZI activation led to
210 STING protein degradation in *WT/SAVI* and *AQ/SAVI* BMDM (Figure 5B). In addition, diABZI
211 treatment caused IκBα degradation in *WT/SAVI* and *AQ/SAVI* BMDM (Figure 5C). Last, using
212 cleavable crosslinker dithiobis(succinimidyl propionate (DSP), we showed that STING in
213 *WT/SAVI, AQ/SAVI* BMDM forms similar dimer *in situ*. Thus, the *AQ/SAVI* BMDM had similar
214 STING degradation, TBK1, IRF3, NFκB activation, and dimerization as the *WT/SAVI* BMDM.

215

216 ***The HAQ* allele increased, and the *AQ* allele restored T-regs in *SAVI(N153S)* mice.**

217 IFNγ was proposed to drive SAVI disease [14,34,48]. We confirmed that *WT/SAVI* CD4 T cells were
218 enriched with IFNγ^+ cells (Figure 6A). However, *WT/SAVI* mice have CD4 T cellpenia. Thus, the
219 total numbers of spleen IFNγ^+ CD4 T cells were comparable in *WT/SAVI* and *AQ/SAVI* mice
220 (Figure 6A). In contrast, the *HAQ/SAVI mice* had decreased IFNγ^+ CD4 T cells (Figure 6A).

221 CD4 T cellpenia depletes CD4 T-regs. Indeed, *WT/SAVI* mice had ~20-fold reduction of spleen
222 FoxP3$^+$ T-regs compared to *AQ/SAVI* or *WT/WT* mice (Figure 6B). The *HAQ/SAVI* mice also had
223 ~10-fold more T-regs than the *WT/SAVI* mice (Figure 6B).

224

225 **Discussion**

226 This study, using the *HAQ, AQ, SAVI(N153S) TMEM173* knock-in mice, reveals the *in vivo*
227 significance of STING-mediated CD4 T cell death. *HAQ, AQ* alleles prevent CD4 T cellpenia, and
228 increase/restore CD4 T-regs in SAVI mice. The results are consistent with previous finding that
229 the impaired CD4 T cell proliferation by the *SAVI(V155M)* mutant could be rescued by the addition
230 of the *HAQ* allele *in vitro* [23]. Besides SAVI, STING has been increasingly implicated in
231 inflammatory diseases such as nonalcoholic fatty liver disease, nonalcoholic steatohepatitis,
232 cardiomyopathy, obesity, diabetes, neurodegenerative diseases, aging, and kidney injury, many of
233 which are independent of type I IFNs [2,3,9]. It is tempting to suggest that STING activation in CD4
234 T cells leads to CD4 T-regs depletion that break tissue tolerance and exacerbates tissue
235 inflammation.

236 Human immunodeficiency virus (HIV) primarily infects CD4 T cells and might activate the
237 STING pathway in CD4 T cells [49-54]. The loss of CD4 T cells is the hallmark of untreated HIV
238 infection [55,56], and the measurement of CD4 T cell count is a central part of HIV care. We found
239 that *HAQ* and *AQ* CD4 T cells are resistant to STING-mediated cell death. Mogensen and
240 colleagues reported that *HAQ/HAQ* was enriched in HIV-infected long-term nonprogressors [39].
241 These *HAQ/HAQ* individuals had reduced inhibition of CD4 T cell proliferation and a reduced
242 immune response to DNA and HIV [39]. It is likely that HIV infection activates STING-cell death
243 pathway in CD4 T cells. Furthermore, in *HAQ/SAVI* and *AQ/SAVI* mice, one copy of *HAQ*, *AQ*
244 allele suppressed CD4 T cell death. *HAQ*, *AQ* carriers might have fewer HIV-induced CD4 T cell
245 death and be long-term nonprogressors in HIV infection-induced Acquired immunodeficiency
246 syndrome (AIDS).

247 Activating the STING pathway is a promising strategy for cancer immunotherapy [57-63].
248 Multiple STING agonists are in clinical trials [44,45]. Recently, the safety issue emerged in some
249 STING agonist trials [44,45]. For example, in the STING agonist, ADU-S100, clinical trial, Grade 3/4
250 treatment-related adverse events were reported in 12.2% of 41 pretreated patients
251 (NCT02675439)[44,45]. The National Institutes of Health defines grade 3 as "incapacitating; unable
252 to perform usual activities; requires absenteeism or bed rest." In a clinical trial using STING
253 antibody-drug-conjugate (ADC) that conjugates diABZI to anti-HER2 Ab, a Grade 5 (fatal)
254 serious adverse event was recorded and deemed related to the STING-ADC (NCT05514717).
255 SAVI disease, driven by overreacting STING, is often fatal. *AQ*, to a less degree, *HAQ*, suppress

256 mortality in SAVI mice. Future STING clinical trials should be based on human *TMEM173*
257 genotype to achieve safe and effective responses.

258 Mechanistically, apoptosis, pyroptosis, ferroptosis, necroptosis, and PANoptosis have all been
259 reported in STING-mediated cell death [24-30,42,43]. Different cell types and STING agonists used
260 likely contributed to the inconsistency and complexity. Here, we focused on lymphopenia in the
261 SAVI mice that avoids ligand-dependent, non-physiological dosage in STING-mediated cell
262 death. *HAQ* and *AQ* alleles could prevent CD4 T cellpenia in the SAVI mice strongly indicating
263 that residue A230 or Q293 prevent STING-mediated CD4 T cell death *in vivo*. Splenocyte from
264 *Q293* mice were resistant to STING agonists-induced cell death *ex vivo*. Thus, it is likely that the
265 Q293 residue is critical for STING-mediate lymphopenia. Notably, Q293 is outside the C-terminal
266 tail (CTT) (residues 341–379 of human STING) critical for TBK1 recruitment and IRF3
267 phosphorylation [64] or miniCTT domain (aa343–354) [23] , or the UPR motif (aa322–343) [46]
268 important for T cells death *in vitro*. Further studies are needed to understand how the aa293 of
269 STING mediates cell death *in vivo*. Noteworthy, *AQ/SAVI* cells had similar TBK1-IRF3, NFκB
270 activation and STING degradation as the *WT/SAVI* cells. Yet, *AQ/SAVI* mice did not have CD4 T
271 cellpenia as *WT/SAVI* mice suggesting that the canonical STING-TBK1-IRF3/NFκB pathway,
272 likely STING oligomerization, is not sufficient for the induction of cell death at the physiological
273 condition.

274 We used the *WT/N153S* knock-in SAVI mouse model that spontaneously develop lung
275 inflammation, T cell cytopenia, and early mortality, mimicking pathological findings in human
276 SAVI patients[15]. Using the *WT/N153S* SAVI mouse model and human Jurkat T cell line, it was
277 proposed that STING activation causes chronic ER stress and unfolded protein response, leading
278 to T cell death by apoptosis [46]. Furthermore, the study showed that crossing *WT/N153S* mice to the
279 OT-I mice reduced ER stress and restored $CD8^+$, but not $CD4^+$, T cells [46]. The restoration of $CD8^+$T
280 cells reduces inflammation and lung disease [46]. However, human *WT/N154S* SAVI patients have
281 normal $CD8^+$ T cells numbers [12], and primary human $CD8^+$ T cells are largely resistant to STING-
282 agonists-induced cell death *ex vivo* (Figure 2A) [24]. Thus, it is puzzling how restoring $CD8^+$ T cells
283 can rescue SAVI phenotypes since the SAVI patients already have normal $CD8^+$ T cells numbers.

284 Finally, it is unexpected that both *HAQ* and *AQ* alleles are resistant to cell death. Our previous
285 studies showed that the *HAQ* and *AQ* alleles have opposite functions [33]. AQ-STING, not HAQ-
286 STING, responds to CDNs [31-33,36-40,65]. *AQ* mice are lean while *HAQ* mice are fat [33]. Most

importantly, *HAQ* was positively selected, while *AQ* was negatively selected, in modern humans outside Africans [33]. Thus, the death pathway of STING is also distinct from the STING function that was naturally selected. Together, we propose that there are at least three unique pathways of STING/MPYS: STING-Type I IFNs, STING-cell death, and STING-fatty acid metabolism.

Materials and Methods

Study Design. The study was designed to reveal (i) the *in vivo* significance of the type I IFNs-independent, STING-dependent cell death function; (ii) the interplay between common *STING* alleles *HAQ, AQ* and the rare, gain-of-function SAVI STING mutation; (iii). The driver for the inflammatory SAVI disease. Mouse splenocytes, primary human lung cells, human THP-1 cells and *HAQ, AQ, SAVI* knock-in mice were used to establish the *in vivo* significance and human relevance. All the repeats were biological replications that involve the same experimental procedures on different mice. Where possible, treatments were assigned blindly to the experimenter by another individual in the lab. When comparing samples from different groups, samples from each group were analyzed in concert, thereby preventing any biases that might arise from analyzing individual treatments on different days. All experiments were repeated at least twice.

Mice. *WT/SAVI(N153S)* mice were purchased from The Jackson Laboratory. *HAQ*, *AQ* mice were previously generated in the lab [32,33]. The *Q293* mice were generated by Cyagen Biosciences. Briefly, the linearized targeting vector was transfected into JM8A3.N1 C57BL/6N embryonic stem cells. A positive embryonic stem clone was subjected to the generation of chimera mice by injection using C57BL/6J blastocysts as the host. Successful germline transmission was confirmed by PCR sequencing. The heterozygous mice were bred to Actin-flpase mice [The Jackson Laboratory, B6.Cg-Tg (ACTFLPe)9205Dym/J] to remove the neo gene and make the *Q293* knock-in mouse. Age- and gender-matched mice (2 – 6 month old, both male and female) were used for indicated experiments. *WT/SAVI* (male) x *WT/HAQ* (female), *WT/SAVI* (male) x *WT/AQ* (female) breeders were set up to generate *HAQ/SAVI*, *AQ/SAVI* mice. Mice were housed at 22°C under a 12-h light-dark cycle with ad libitum access to water and a chow diet (3.1 kcal/g, Teklad 2018, Envigo, Sommerset, NJ) and bred under pathogen-free conditions in the Animal Research Facility at the University of Florida. Littermates of the same sex were randomly assigned to experimental groups. All mouse experiments were performed by the regulations and approval of the Institutional Animal Care and Use Committee at the University of Florida, IACUC202200000058.

322 **Reagents.** Recombinant human IFNβ (R&D, cat no. 8499-IF-010/CF), diABZI (Invivogen, cat no.
323 2138299-34-8), 2'3'-cGAMP (Invivogen, cat no. tlrl-nacga23-02), DMXAA (Invivogen, cat no.
324 tlrl-dmx), H151 (Invivogen, cat no. inh-h151), RpRpSSCDA (Biolog, cat no. C118), THP1-
325 Dual™ KO-STING Cells (Invivogen, cat no. thpd-kostg). All other chemical inhibitors are from
326 Selleckchem.
327
328 **Histology.** Lungs and livers were fixed in 10% formalin, paraffin-embedded, and cut into 4-µm
329 sections. Lung, liver sections were then stained for hematoxylin-eosin. All staining procedures
330 were performed by the histology core at the University of Florida. Briefly, tissue sectins were
331 immersed Harris Hematoxylin for 10 seconds, then washed with tap water. Cleard sections were
332 re-immersed in EOSIN stain for ~30 seconds. The sections were washed with tap water until clear,
333 then dehydrate in ascending alcohol solutions (50%,70%,80%,95% x 2, 100% x 2). Afterwards,
334 the sections werer cleared with xylene (3 - 4 x). The sections were mounted on glass slide with
335 permount organic mounting medium for visulization.
336
337 **Lung Function.** Pulmonary function was evaluated using an isolated, buffer-perfused mouse lung
338 apparatus (Hugo Sachs Elektronik, March-Huggstetten, Germany), as previously described [66].
339 Briefly, mice were anesthetized with ketamine and xylazine and a tracheostomy was performed,
340 and animals were ventilated with room air at 100 breaths/min at a tidal volume of 7 µl/g body
341 weight with a positive end-expiratory pressure of 2 cm H2O using a pressure-controlled ventilator
342 (Hugo Sachs Elektronik, March-Huggstetten, Germany).
343
344 **Isolation of lung cells.** Cells were isolated from the lung as previously described [67]. The lungs
345 were perfused with ice-cold PBS and removed. Lungs were digested in DMEM containing
346 200µg/ml DNase I (Roche, 10104159001), 25µg/ml Liberase TM (Roche, 05401119001) at 37°C
347 for 2 hours. Red blood cells were then lysed and a single cell suspension was prepared by filtering
348 through a 70-µm cell strainer.
349
350 **BMDM activation**
351 BMDMs were induced from mouse bone marrow cells cultured in RPMI 1640 (cat#11965;
352 Invitrogen) with 10% FBS, 2 mM L-glutamine, 1 mM sodium pyruvate, 10 mM HEPES buffer,

353 1% nonessential amino acids, 50 mM 2-ME, 1% Pen/Strep, with 20ng/ml M-CSF (Kingfisher,
354 RP0407M) for 10 days [32].
355
356 **Flow cytometry.** Single cell suspensions were stained with fluorescent-dye-conjugated antibodies
357 in PBS containing 2% FBS and 1mM EDTA. Surface stains were performed at 4°C for 20 min.
358 For intracellular cytokine or transcription factor staining of murine and human cells, cells were
359 fixed and permeabilized with the Foxp3 staining buffer set (eBioscience, cat no 00-5523-00). Cells
360 were washed and stained with surface markers. Cells were then fixed and permeabilized
361 (eBioscience, cat no. 00-5523-00) for intracellular cytokine stain. Data were acquired on a BD
362 LSRFortessa and analyzed using the FlowJo software package (FlowJo, LLC). Cell sorting was
363 performed on the BD FACSAriaIII Flow Cytometer and Cell Sorter. More information on the
364 antibodies used can be found in supplementary table S1.
365
366 **Human lung explants**
367 Human lung explants were procured at the Lung Transplant Center, Division of Pulmonary,
368 Critical Care and Sleep Medicine, Department of Medicine, University of Florida. Donor and
369 patients consent was obtained for a research protocol (UF IRB201902955-Treatment with IFNβ
370 Induces Tolerogenic Lung Dendritic Cells in Human advanced lung disease). Healthy donor lungs
371 were surgically removed postmortem, perfused, small pieces were cut from the right middle and
372 lower lobes for research purpose, and stored in cold Perfadex ® at 4°C for no more than 12 hrs
373 before processing. Ex planted lungs from emphysema lung transplant patients were stored in cold
374 Perfadex ® at 4°C for no more than 12 hrs before the process. No lung explants were procured
375 from prisoners.
376
377 **Statistical Analysis.** To gain statistical power, we employ three~four mice/groups to characterize
378 lung immunity. The statistical justification for group size was calculated using the SAS program
379 to calculate the animal numbers. The analysis was carried out using a standard error of 0.5 for
380 immunological assays, and a power of 0.9. All data are expressed as means ± SEM. Statistical
381 significance was evaluated using Prism 7.0 software. Comparisons between two groups were
382 analyzed by performing an unpaired Student's *t* test. Comparisons between more than two groups

383 were analyzed by performing a one-way analysis of variance (ANOVA) with Tukey's multiple
384 comparisons test.

385 **Supplemental materials**

386 Figure S1: Bx-795 inhibits diABZI-induced mouse splenocyte death.

387 Figure S2: STING activation in primary human cells and THP-1 cells reconstituted with WT
388 human STING.

389 Figure S3: *HAQ* and *AQ* restore bone marrow monocytes in SAVI(N153S) mice.

390 Figure S4: *HAQ* and *AQ* suppress lung myeloid infiltration in SAVI(N153S) mice.

391

392 References

393 1 Barber, G. N. STING: infection, inflammation and cancer. *Nat Rev Immunol* **15**, 760-770
394 (2015). https://doi.org:10.1038/nri3921

395 2 Skopelja-Gardner, S., An, J. & Elkon, K. B. Role of the cGAS-STING pathway in systemic
396 and organ-specific diseases. *Nat Rev Nephrol* **18**, 558-572 (2022).
397 https://doi.org:10.1038/s41581-022-00589-6

398 3 Bai, J. & Liu, F. cGASSTING signaling and function in metabolism and kidney diseases.
399 *J Mol Cell Biol* **13**, 728-738 (2021). https://doi.org:10.1093/jmcb/mjab066

400 4 Li, H., Guo, X., Aquino, E. & Wu, C. Mini review: STING activation during non-alcoholic
401 fatty liver disease. *Front Nutr* **10**, 1139339 (2023).
402 https://doi.org:10.3389/fnut.2023.1139339

403 5 Gulen, M. F. *et al.* cGAS-STING drives ageing-related inflammation and
404 neurodegeneration. *Nature* **620**, 374-380 (2023). https://doi.org:10.1038/s41586-023-
405 06373-1

406 6 Szego, E. M. *et al.* Constitutively active STING causes neuroinflammation and
407 degeneration of dopaminergic neurons in mice. *Elife* **11** (2022).
408 https://doi.org:10.7554/eLife.81943

409 7 Gao, L. *et al.* STING/ACSL4 axis-dependent ferroptosis and inflammation promote
410 hypertension-associated chronic kidney disease. *Mol Ther* (2023).
411 https://doi.org:10.1016/j.ymthe.2023.07.026

412 8 Yan, M. *et al.* Mitochondrial damage and activation of the cytosolic DNA sensor cGAS-
413 STING pathway lead to cardiac pyroptosis and hypertrophy in diabetic cardiomyopathy
414 mice. *Cell Death Discov* **8**, 258 (2022). https://doi.org:10.1038/s41420-022-01046-w

415 9 Gao, K. M., Marshak-Rothstein, A. & Fitzgerald, K. A. Type-1 interferon-dependent and
416 -independent mechanisms in cyclic GMP-AMP synthase-stimulator of interferon genes-
417 driven auto-inflammation. *Curr Opin Immunol* **80**, 102280 (2023).
418 https://doi.org:10.1016/j.coi.2022.102280

419 10 Yamashiro, L. H. *et al.* Interferon-independent STING signaling promotes resistance to
420 HSV-1 in vivo. *Nat Commun* **11**, 3382 (2020). https://doi.org:10.1038/s41467-020-17156-
421 x

422 11 Wu, J., Dobbs, N., Yang, K. & Yan, N. Interferon-Independent Activities of Mammalian
423 STING Mediate Antiviral Response and Tumor Immune Evasion. *Immunity* **53**, 115-126
424 e115 (2020). https://doi.org:10.1016/j.immuni.2020.06.009

425 12 Liu, Y. *et al.* Activated STING in a vascular and pulmonary syndrome. *N Engl J Med* **371**,
426 507-518 (2014). https://doi.org:10.1056/NEJMoa1312625

427 13 Luksch, H. *et al.* STING-associated lung disease in mice relies on T cells but not type I
428 interferon. *J Allergy Clin Immunol* **144**, 254-266 e258 (2019).
429 https://doi.org:10.1016/j.jaci.2019.01.044

430 14 Stinson, W. A. *et al.* The IFN-gamma receptor promotes immune dysregulation and disease
431 in STING gain-of-function mice. *JCI Insight* **7** (2022).
432 https://doi.org:10.1172/jci.insight.155250

433 15 Warner, J. D. *et al.* STING-associated vasculopathy develops independently of IRF3 in
434 mice. *J Exp Med* **214**, 3279-3292 (2017). https://doi.org:10.1084/jem.20171351

435 16 Fremond, M. L. *et al.* Overview of STING-Associated Vasculopathy with Onset in Infancy
436 (SAVI) Among 21 Patients. *J Allergy Clin Immunol Pract* **9**, 803-818 e811 (2021).
437 https://doi.org:10.1016/j.jaip.2020.11.007

438 17 Rodero, M. P. *et al.* Type I interferon-mediated autoinflammation due to DNase II
439 deficiency. *Nat Commun* **8**, 2176 (2017). https://doi.org:10.1038/s41467-017-01932-3

440 18 Li, T. *et al.* TBK1 recruitment to STING mediates autoinflammatory arthritis caused by
441 defective DNA clearance. *J Exp Med* **219** (2022). https://doi.org:10.1084/jem.20211539

442 19 Yum, S., Li, M., Fang, Y. & Chen, Z. J. TBK1 recruitment to STING activates both IRF3
443 and NF-kappaB that mediate immune defense against tumors and viral infections. *Proc*
444 *Natl Acad Sci U S A* **118** (2021). https://doi.org:10.1073/pnas.2100225118

445 20 Gaidt, M. M. *et al.* The DNA Inflammasome in Human Myeloid Cells Is Initiated by a
446 STING-Cell Death Program Upstream of NLRP3. *Cell* **171**, 1110-1124 e1118 (2017).
447 https://doi.org:10.1016/j.cell.2017.09.039

448 21 Jin, L. *et al.* STING/MPYS mediates host defense against Listeria monocytogenes
449 infection by regulating Ly6C(hi) monocyte migration. *J Immunol* **190**, 2835-2843 (2013).
450 https://doi.org:10.4049/jimmunol.1201788

451 22 Larkin, B. *et al.* Cutting Edge: Activation of STING in T Cells Induces Type I IFN
452 Responses and Cell Death. *J Immunol* **199**, 397-402 (2017).
453 https://doi.org:10.4049/jimmunol.1601999

454 23 Cerboni, S. *et al.* Intrinsic antiproliferative activity of the innate sensor STING in T
455 lymphocytes. *J Exp Med* **214**, 1769-1785 (2017). https://doi.org:10.1084/jem.20161674

456 24 Kuhl, N. *et al.* STING agonism turns human T cells into interferon-producing cells but
457 impedes their functionality. *EMBO Rep* **24**, e55536 (2023).
458 https://doi.org:10.15252/embr.202255536

459 25 Jin, L. *et al.* MPYS, a novel membrane tetraspanner, is associated with major
460 histocompatibility complex class II and mediates transduction of apoptotic signals. *Mol*
461 *Cell Biol* **28**, 5014-5026 (2008). https://doi.org:10.1128/MCB.00640-08

462 26 Gulen, M. F. *et al.* Signalling strength determines proapoptotic functions of STING. *Nat*
463 *Commun* **8**, 427 (2017). https://doi.org:10.1038/s41467-017-00573-w

464 27 Kabelitz, D. *et al.* Signal strength of STING activation determines cytokine plasticity and
465 cell death in human monocytes. *Sci Rep* **12**, 17827 (2022). https://doi.org:10.1038/s41598-
466 022-20519-7

467 28 Murthy, A. M. V., Robinson, N. & Kumar, S. Crosstalk between cGAS-STING signaling
468 and cell death. *Cell Death Differ* **27**, 2989-3003 (2020). https://doi.org:10.1038/s41418-
469 020-00624-8

470 29 Li, C., Liu, J., Hou, W., Kang, R. & Tang, D. STING1 Promotes Ferroptosis Through
471 MFN1/2-Dependent Mitochondrial Fusion. *Front Cell Dev Biol* **9**, 698679 (2021).
472 https://doi.org:10.3389/fcell.2021.698679

473 30 Song, C. *et al.* SHR1032, a novel STING agonist, stimulates anti-tumor immunity and
474 directly induces AML apoptosis. *Sci Rep* **12**, 8579 (2022). https://doi.org:10.1038/s41598-
475 022-12449-1

476 31 Jin, L. *et al.* Identification and characterization of a loss-of-function human MPYS variant.
477 *Genes Immun* **12**, 263-269 (2011). https://doi.org:10.1038/gene.2010.75

478 32 Patel, S. *et al.* The Common R71H-G230A-R293Q Human TMEM173 Is a Null Allele. *J*
479 *Immunol* **198**, 776-787 (2017). https://doi.org:10.4049/jimmunol.1601585

480 33 Mansouri, S. *et al.* MPYS Modulates Fatty Acid Metabolism and Immune Tolerance at
481 Homeostasis Independent of Type I IFNs. *J Immunol* **209**, 2114-2132 (2022).
482 https://doi.org:10.4049/jimmunol.2200158

483 34 Patel, S. & Jin, L. TMEM173 variants and potential importance to human biology and
484 disease. *Genes Immun* **20**, 82-89 (2019). https://doi.org:10.1038/s41435-018-0029-9

485 35 Liu, Y. *et al.* Activated STING in a vascular and pulmonary syndrome. *N Engl J Med* **371**,
486 507-518 (2014). https://doi.org:10.1056/NEJMoa1312625

487 36 Sebastian, M. *et al.* Obesity and STING1 genotype associate with 23-valent pneumococcal
488 vaccination efficacy. *JCI Insight* **5** (2020). https://doi.org:10.1172/jci.insight.136141

489 37 Yi, G. *et al.* Single nucleotide polymorphisms of human STING can affect innate immune
490 response to cyclic dinucleotides. *PLoS One* **8**, e77846 (2013).
491 https://doi.org:10.1371/journal.pone.0077846

492 38 Patel, S. *et al.* Response to Comment on "The Common R71H-G230A-R293Q Human
493 TMEM173 Is a Null Allele". *J Immunol* **198**, 4185-4188 (2017).
494 https://doi.org:10.4049/jimmunol.1700322

495 39 Nissen, S. K. *et al.* Multiple Homozygous Variants in the STING-Encoding TMEM173
496 Gene in HIV Long-Term Nonprogressors. *J Immunol* **200**, 3372-3382 (2018).
497 https://doi.org:10.4049/jimmunol.1701284

498 40 Ruiz-Moreno, J. S. *et al.* The common HAQ STING variant impairs cGAS-dependent
499 antibacterial responses and is associated with susceptibility to Legionnaires' disease in
500 humans. *PLoS Pathog* **14**, e1006829 (2018). https://doi.org:10.1371/journal.ppat.1006829

501 41 Ramanjulu, J. M. *et al.* Design of amidobenzimidazole STING receptor agonists with
502 systemic activity. *Nature* **564**, 439-443 (2018). https://doi.org:10.1038/s41586-018-0705-
503 y

504 42 Messaoud-Nacer, Y. *et al.* STING agonist diABZI induces PANoptosis and DNA mediated
505 acute respiratory distress syndrome (ARDS). *Cell Death Dis* **13**, 269 (2022).
506 https://doi.org:10.1038/s41419-022-04664-5

507 43 Tang, C. H. *et al.* Agonist-Mediated Activation of STING Induces Apoptosis in Malignant
508 B Cells. *Cancer Res* **76**, 2137-2152 (2016). https://doi.org:10.1158/0008-5472.CAN-15-
509 1885

510 44 Meric-Bernstam, F. *et al.* Combination of the STING Agonist MIW815 (ADU-S100) and
511 PD-1 Inhibitor Spartalizumab in Advanced/Metastatic Solid Tumors or Lymphomas: An
512 Open-Label, Multicenter, Phase Ib Study. *Clin Cancer Res* **29**, 110-121 (2023).
513 https://doi.org:10.1158/1078-0432.CCR-22-2235

514 45 Meric-Bernstam, F. *et al.* Phase I Dose-Escalation Trial of MIW815 (ADU-S100), an
515 Intratumoral STING Agonist, in Patients with Advanced/Metastatic Solid Tumors or
516 Lymphomas. *Clin Cancer Res* **28**, 677-688 (2022). https://doi.org:10.1158/1078-
517 0432.CCR-21-1963

518 46 Wu, J. *et al.* STING-mediated disruption of calcium homeostasis chronically activates ER
519 stress and primes T cell death. *J Exp Med* **216**, 867-883 (2019).
520 https://doi.org:10.1084/jem.20182192

521 47 Motwani, M. *et al.* Hierarchy of clinical manifestations in SAVI N153S and V154M mouse
522 models. *Proc Natl Acad Sci U S A* **116**, 7941-7950 (2019).
523 https://doi.org:10.1073/pnas.1818281116

524 48 Gao, K. M., Motwani, M., Tedder, T., Marshak-Rothstein, A. & Fitzgerald, K. A.
525 Radioresistant cells initiate lymphocyte-dependent lung inflammation and IFNgamma-
526 dependent mortality in STING gain-of-function mice. *Proc Natl Acad Sci U S A* **119**,
527 e2202327119 (2022). https://doi.org:10.1073/pnas.2202327119

528 49 Monroe, K. M. *et al.* IFI16 DNA sensor is required for death of lymphoid CD4 T cells
529 abortively infected with HIV. *Science* **343**, 428-432 (2014).
530 https://doi.org:10.1126/science.1243640

531 50 Doitsh, G. *et al.* Cell death by pyroptosis drives CD4 T-cell depletion in HIV-1 infection.
532 *Nature* **505**, 509-514 (2014). https://doi.org:10.1038/nature12940

533 51 Jakobsen, M. R., Olagnier, D. & Hiscott, J. Innate immune sensing of HIV-1 infection.
534 *Curr Opin HIV AIDS* **10**, 96-102 (2015). https://doi.org:10.1097/COH.0000000000000129

535 52 Silvin, A. & Manel, N. Innate immune sensing of HIV infection. *Curr Opin Immunol* **32**,
536 54-60 (2015). https://doi.org:10.1016/j.coi.2014.12.003

537 53 Altfeld, M. & Gale, M., Jr. Innate immunity against HIV-1 infection. *Nat Immunol* **16**, 554-
538 562 (2015). https://doi.org:10.1038/ni.3157

539 54 Krapp, C., Jonsson, K. & Jakobsen, M. R. STING dependent sensing - Does HIV actually
540 care? *Cytokine Growth Factor Rev* **40**, 68-76 (2018).
541 https://doi.org:10.1016/j.cytogfr.2018.03.002

542 55 Gubser, C., Pitman, M. C. & Lewin, S. R. CD4(+) T cell signatures in HIV infection. *Nat*
543 *Immunol* **20**, 948-950 (2019). https://doi.org:10.1038/s41590-019-0447-5

544 56 Morou, A. *et al.* Altered differentiation is central to HIV-specific CD4(+) T cell
545 dysfunction in progressive disease. *Nat Immunol* **20**, 1059-1070 (2019).
546 https://doi.org:10.1038/s41590-019-0418-x

547 57 Hines, J. B., Kacew, A. J. & Sweis, R. F. The Development of STING Agonists and
548 Emerging Results as a Cancer Immunotherapy. *Curr Oncol Rep* **25**, 189-199 (2023).
549 https://doi.org:10.1007/s11912-023-01361-0

550 58 Samson, N. & Ablasser, A. The cGAS-STING pathway and cancer. *Nat Cancer* **3**, 1452-
551 1463 (2022). https://doi.org:10.1038/s43018-022-00468-w

552 59 Liu, Y. *et al.* STING, a promising target for small molecular immune modulator: A review.
553 *Eur J Med Chem* **211**, 113113 (2021). https://doi.org:10.1016/j.ejmech.2020.113113

554 60 Zheng, J. *et al.* Comprehensive elaboration of the cGAS-STING signaling axis in cancer
555 development and immunotherapy. *Mol Cancer* **19**, 133 (2020).
556 https://doi.org:10.1186/s12943-020-01250-1

557 61 Corrales, L. *et al.* Direct Activation of STING in the Tumor Microenvironment Leads to
558 Potent and Systemic Tumor Regression and Immunity. *Cell Rep* **11**, 1018-1030 (2015).
559 https://doi.org:10.1016/j.celrep.2015.04.031

560 62 Fu, J. *et al.* STING agonist formulated cancer vaccines can cure established tumors
561 resistant to PD-1 blockade. *Sci Transl Med* **7**, 283ra252 (2015).
562 https://doi.org:10.1126/scitranslmed.aaa4306

563 63 Barber, G. N. Innate immune DNA sensing pathways: STING, AIMII and the regulation
564 of interferon production and inflammatory responses. *Curr Opin Immunol* **23**, 10-20
565 (2011). https://doi.org:10.1016/j.coi.2010.12.015

566 64 Liu, S. *et al.* Phosphorylation of innate immune adaptor proteins MAVS, STING, and TRIF
567 induces IRF3 activation. *Science* **347**, aaa2630 (2015).
568 https://doi.org:10.1126/science.aaa2630

569 65 Movert, E. *et al.* Interplay between human STING genotype and bacterial NADase activity
570 regulates inter-individual disease variability. *Nat Commun* **14**, 4008 (2023).
571 https://doi.org:10.1038/s41467-023-39771-0

572 66 Cai, J. *et al.* MicroRNA-206 antagomiRenriched extracellular vesicles attenuate lung
573 ischemiareperfusion injury through CXCL1 regulation in alveolar epithelial cells. *J Heart*
574 *Lung Transplant* **39**, 1476-1490 (2020). https://doi.org:10.1016/j.healun.2020.09.012

575 67 Mansouri, S. *et al.* Lung IFNAR1(hi) TNFR2(+) cDC2 promotes lung regulatory T cells
576 induction and maintains lung mucosal tolerance at steady state. *Mucosal Immunol* **13**, 595-
577 608 (2020). https://doi.org:10.1038/s41385-020-0254-1

578

579

Acknowledgments This work was supported by NIH grants HL152163 (to L.J.).

Author contributions L.J. conceived and designed the research. A.A.T, L.A.S, A.T.P, A.K.S, A, J,B, L.J. performed experiments and analyzed the data. A.M.E helped with human lung explants. L.J. wrote the manuscript. L.J. supervised the overall research.

Competing interests, The authors declare that they have no competing interests.

Data and materials availability All data needed to evaluate the conclusions in the paper are present in the paper or the supplementary materials.

588 **Figure Captions**

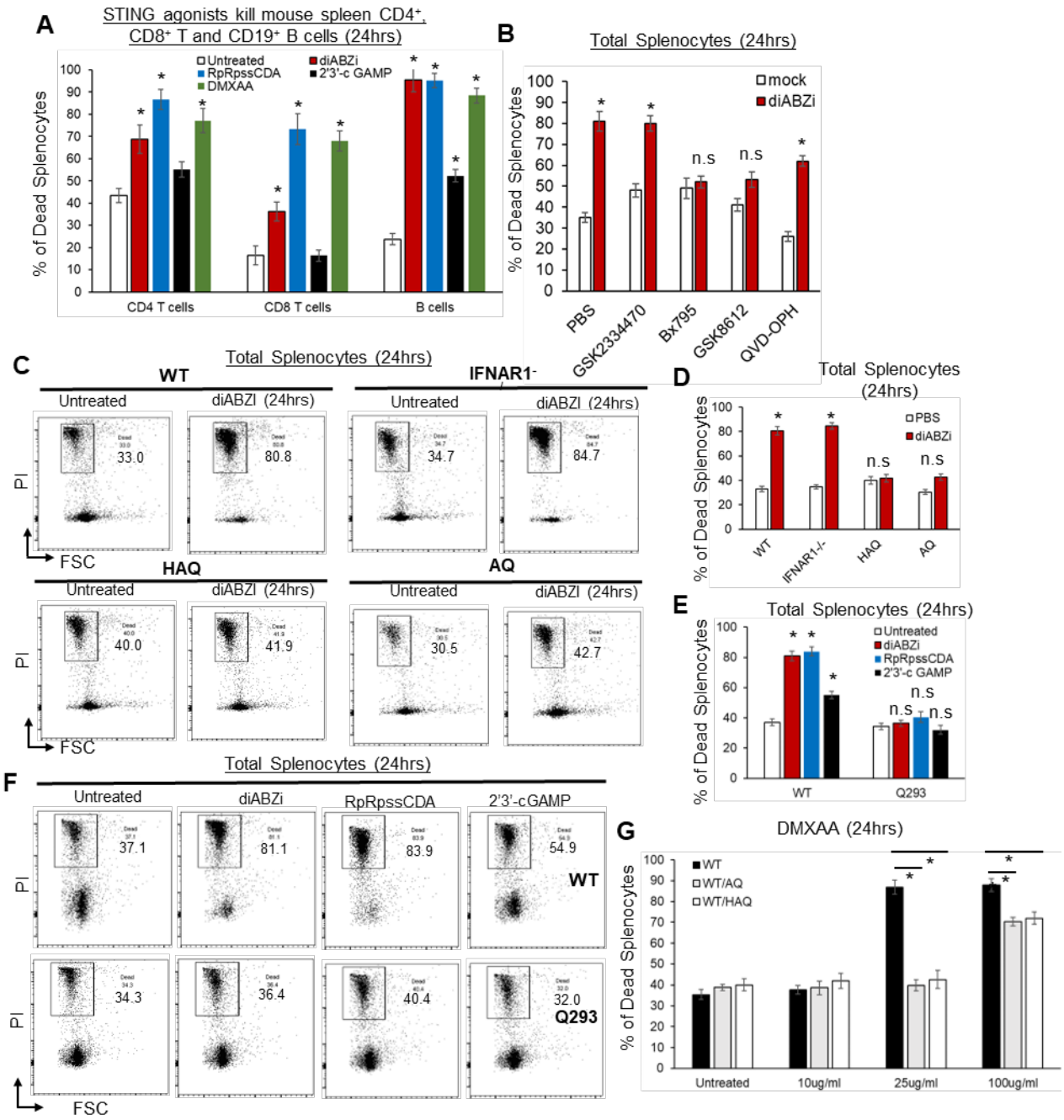

589

590 **Figure 1. Splenocytes from *HAQ*, *AQ*, and *Q293* mice are resistant to STING-mediated cell**

591 **death *ex vivo*. A.** C57BL/6N splenocytes were treated directly (no transfection) with diABZI

592 (100ng/ml), RpRpssCDA (5 µg/ml) or 2′3′-cGAMP (10µg/ml), DMXAA (25µg/ml) for 24hrs in

593 culture. CD4, CD8 T cells and CD19 B cells death were determined by PI staining. **B**. Splenocytes
594 from C57BL/6N mice were pre-treated with indicated small molecules, GSK2334470 (1.25μM),
595 GSK8612 (2.5μM), Bx-795 (0.5μM), QVD-OPH (25μM) for 2hrs. diABZI (100ng/ml) was added
596 in culture for another 24hrs. Dead cells were determined by PI staining. **C-D.** Flowcytometry of
597 *HAQ*, *AQ*, IFNAR1$^{-/-}$ or C57BL/6N splenocytes treated with diABZI (100ng/ml) for 24hrs. Cell
598 death was determined by PI staining. **E-F**. *Q293* or the *WT* littermates splenocytes were treated
599 with diABZI (100ng/ml), RpRpssCDA (5 μg/ml) or 2′3′-cGAMP 10μg/ml) for 24h. Cell death was
600 determined by PI staining. **G.** *WT/HAQ*, *WT/AQ*, or *WT/WT* littermates splenocytes were treated
601 with DMXAA (10, 25 or 100μg/ml) for 24h. Cell death was determined by PI staining. Data are
602 representative of three independent experiments. Graphs represent the mean with error bars
603 indication s.e.m. P values are determined by one-way ANOVA Tukey's multiple comparison test
604 (A, E, G) or unpaired student T-test (B, D). * $p<0.05$. n.s: not significant.

605

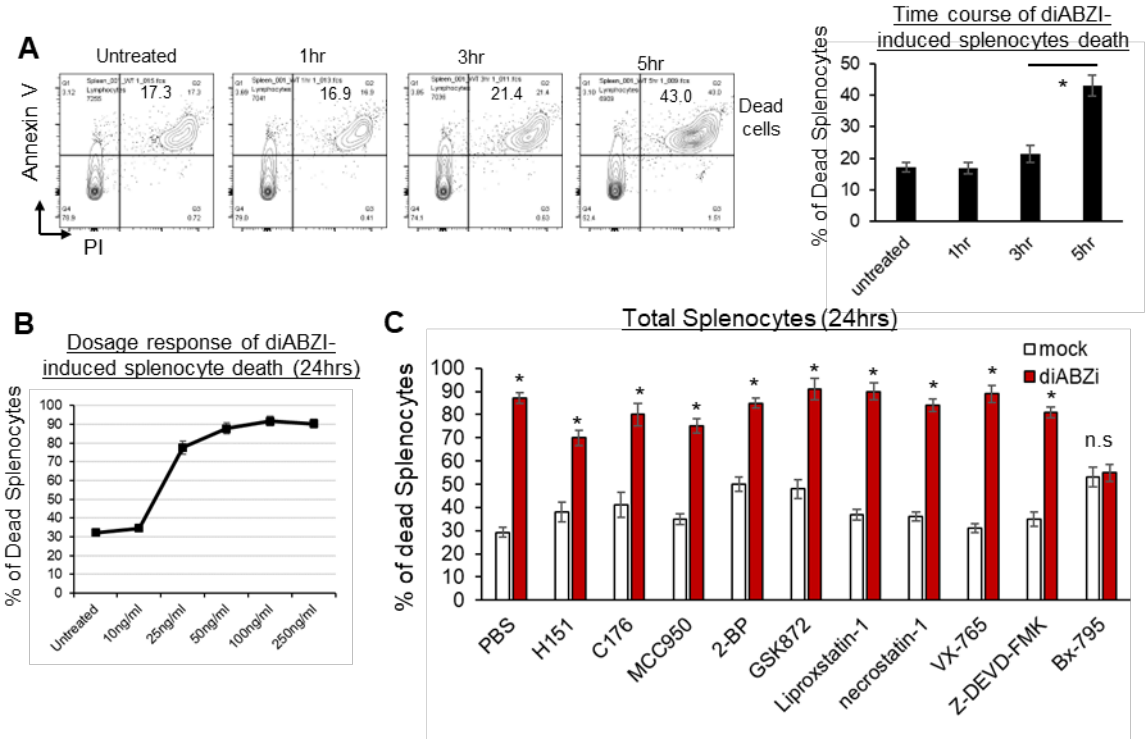

Figure S1. Bx-795 inhibits diABZI-induced mouse splenocyte death. A. Splenocytes from C57BL/6N mice were treated with 100ng/ml diABZI in culture for the indicated time. Dead cells were determined by PI and Annexin V staining. **B.** Splenocytes from C57BL/6N mice were treated with indicated dose of diABZi in culture for 24hrs. Dead cells were determined by PI staining. **C**. Splenocytes from C57BL/6N mice were pre-treated with indicated small molecules, H151 (10µg/ml), C176 (1µM), MCC950 (1.25µM), 2-BP (20µM), GSK872 (312.5nM), Liproxstatin-1 (1µM), necrostatin-1 (10µM), VX-765 (1µM), Z-DEVD-FMK (25µM), Bx-795 (0.5µM) for 2hrs. diABZi (100ng/ml) was added in culture for another 24hrs0 1Dead cells were determined by PI staining. Data are representative of three independent experiments. Graphs represent the mean with error bars indication s.e.m. n=3~5 mice/group. *p* values are determined by one-way ANOVA Tukey's multiple comparison test (A) or unpaired student T-test (C). * $p<0.05$. n.s: not significant.

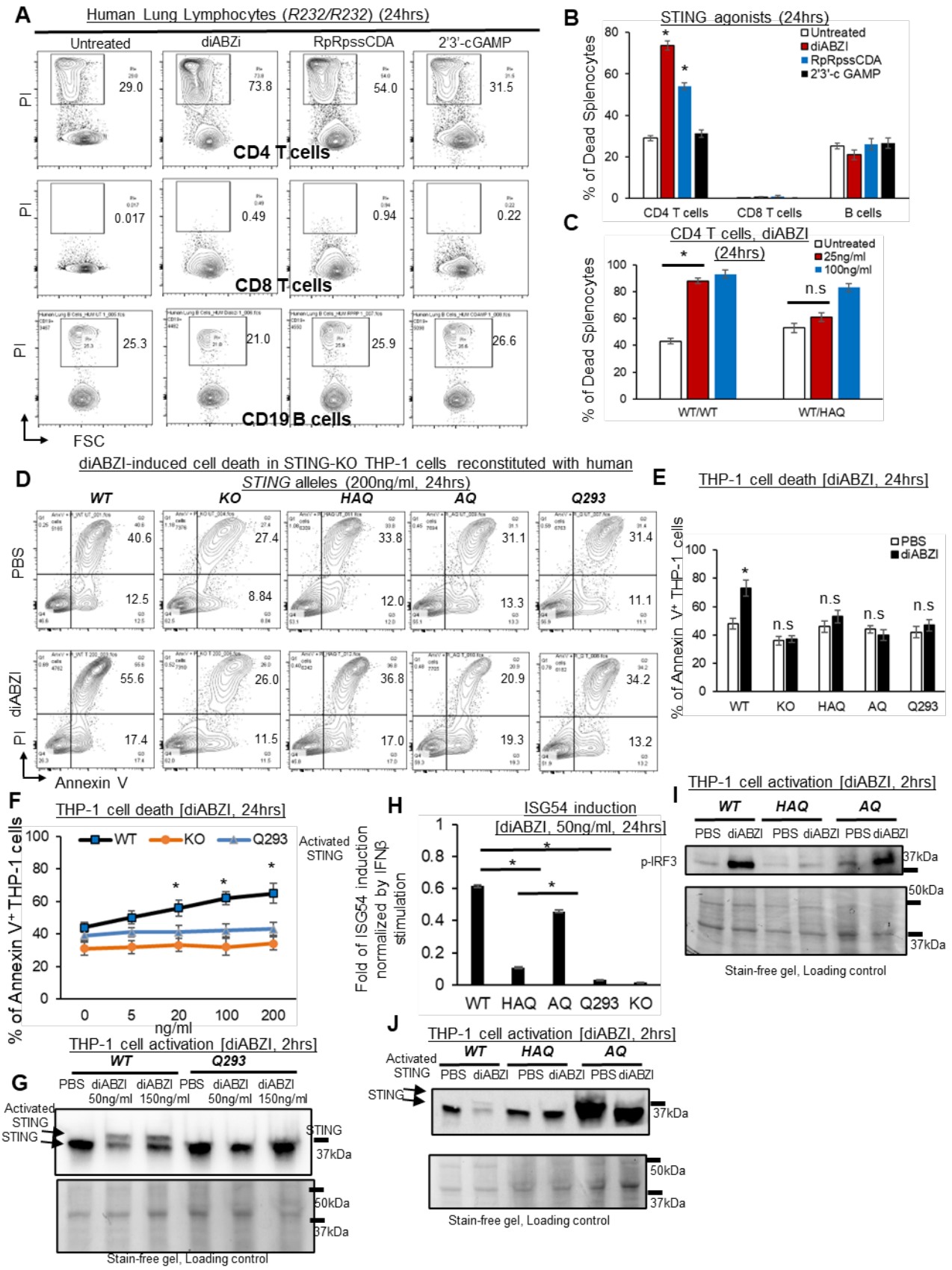
A
Human Lung Lymphocytes (R232/R232) (24hrs)
Untreated
diABZi
RpRpssCDA
2'3'-cGAMP
PI
29.0
73.8
54.0
31.5
CD4 T cells
0.017
0.49
0.94
0.22
CD8 T cells
25.3
21.0
25.9
26.6
CD19 B cells
FSC
B
STING agonists (24hrs)
% of Dead Splenocytes
Untreated
diABZI
RpRpssCDA
2'3'-c GAMP
CD4 T cells
CD8 T cells
B cells
C
CD4 T cells, diABZI (24hrs)
Untreated
25ng/ml
100ng/ml
n.s
WT/WT
WT/HAQ
D
diABZI-induced cell death in STING-KO THP-1 cells reconstituted with human STING alleles (200ng/ml, 24hrs)
WT
KO
HAQ
AQ
Q293
PBS
diABZI
40.6
12.5
27.4
8.84
33.8
12.0
31.1
13.3
31.4
11.1
55.6
17.4
26.0
11.5
36.8
17.0
20.9
19.3
34.2
13.2
Annexin V
E
THP-1 cell death [diABZI, 24hrs]
% of Annexin V+ THP-1 cells
PBS
diABZI
n.s
WT
KO
HAQ
AQ
Q293
F
THP-1 cell death [diABZI, 24hrs]
% of Annexin V+ THP-1 cells
WT
KO
Q293
Activated STING
ng/ml
H
ISG54 induction [diABZI, 50ng/ml, 24hrs]
Fold of ISG54 induction normalized by IFNβ stimulation
WT
HAQ
AQ
Q293
KO
I
THP-1 cell activation [diABZI, 2hrs]
WT
HAQ
AQ
PBS
diABZI
p-IRF3
37kDa
50kDa
Stain-free gel, Loading control
G
THP-1 cell activation [diABZI, 2hrs]
WT
Q293
PBS
diABZI 50ng/ml
diABZI 150ng/ml
Activated STING
STING
37kDa
50kDa
Stain-free gel, Loading control
J
THP-1 cell activation [diABZI, 2hrs]
WT
HAQ
AQ
Activated STING
STING
37kDa
50kDa
Stain-free gel, Loading control

618

619 **Figure 2. *HAQ* , *AQ*, and *Q293* human cells are resistant to STING agonists-induced death.**
620 **A-B.** Total human Lung cells from *WT/WT* individuals were treated with diABZi (100ng/ml) for
621 24hrs. Cell death in CD4, CD8 T cells and CD19 B cells were determined by PI staining. **C**. Total
622 lung cells from a *WT/HAQ* (2 individuals) and a *WT/WT* (3 individuals) were treated with diABZi
623 (25, 100ng/ml) for 24h. Cell death in CD4 T cells was determined by PI staining. **D-E**. STING-
624 KO THP-1 cells (Invivogen,, cat no. thpd-kostg) were stably reconstituted with human *WT (R232),*
625 *HAQ*, *AQ*, *Q293*. Cells were treated with diABZI (200ng/ml) in culture for 24 hrs. Dead cells were
626 determined by Annexin V staining. **F.** STING-KO THP-1 cells stably reconstituted with human
627 *WT (R232), Q293* were treated with indicated dose of diABZI for 24hs in culture. Dead cells were
628 determined by Annexin V staining. G. STING-KO THP-1 cells stably reconstituted with human
629 *WT (R232), Q293* were treated with indicated dose of diABZI for 2hs in culture. STING activation
630 was detected by anti-STING antibody (Proteintech, #19851-1-AP). **H**. STING-KO THP-1 cells
631 stably reconstituted with human *WT (R232), HAQ*, *AQ*, *Q293* were treated with 50ng/ml diABZI
632 in culture for 24hrs. ISG-54 reporter luciferase activity was determined in cell supernatant and
633 normalized to 10ng/ml IFNβ-stimulated ISG-54 luciferase activity. **I-J.** STING-KO THP-1 cells
634 stably reconstituted with human *WT (R232), HAQ*, *AQ* were treated with 50ng/ml diABZI in
635 culture for 2hrs. STING and IRF3 activation were determined by anti-STING antibody and anti-p
636 IRF3 antibody (CST, Ser396, clone 4D4G). Data are representative of at least two independent
637 experiments. Graphs represent the mean with error bars indication s.e.m. *p* values determined by
638 one-way ANOVA Tukey's multiple comparison test (**B, C, F, G**) or unpaired student T-test (**E**).
639 * $p<0.05$, n.s: not significant.

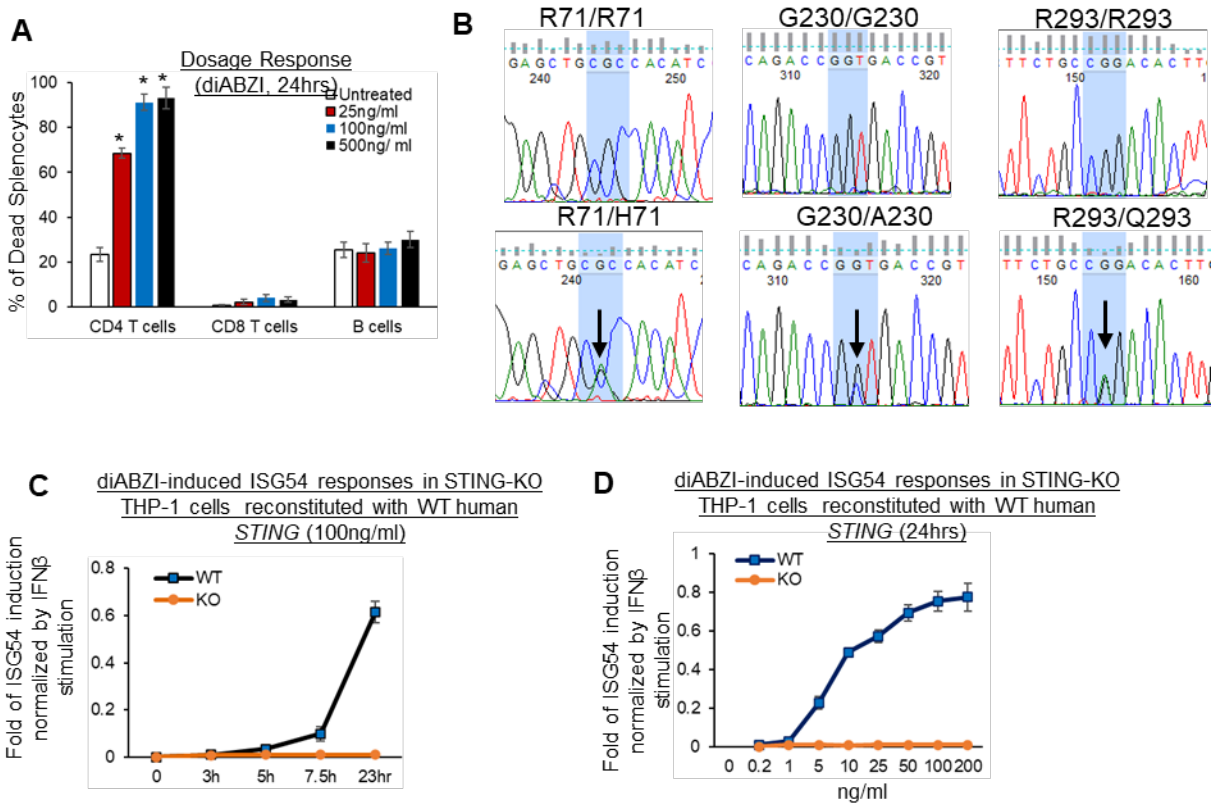

Figure S2. STING activation in primary human cells and THP-1 cells reconstituted with *WT* human *STING*. A. Total human Lung cells from *WT/WT* individuals were treated with indicated dose of diABZi for 24hrs. Cell death in CD4, CD8 T cells and CD19 B cells were determined by PI staining. **B.** Sequencing results of human *TMEM173* gene in *WT/WT* and *WT/HAQ* individuals. **C-D**. STING-KO THP-1 cells stably reconstituted with human *WT (R232)* were treated with indicated dose of diABZI for indicated time in culture. ISG-54 reporter luciferase activity was determined in cell supernatant and normalized to 10ng/ml IFNβ-stimulated ISG-54 luciferase activity. Data are representative of at least two independent experiments. Graphs represent the mean with error bars indication s.e.m. *p* values determined by one-way ANOVA Tukey's multiple comparison test. * $p<0.05$,

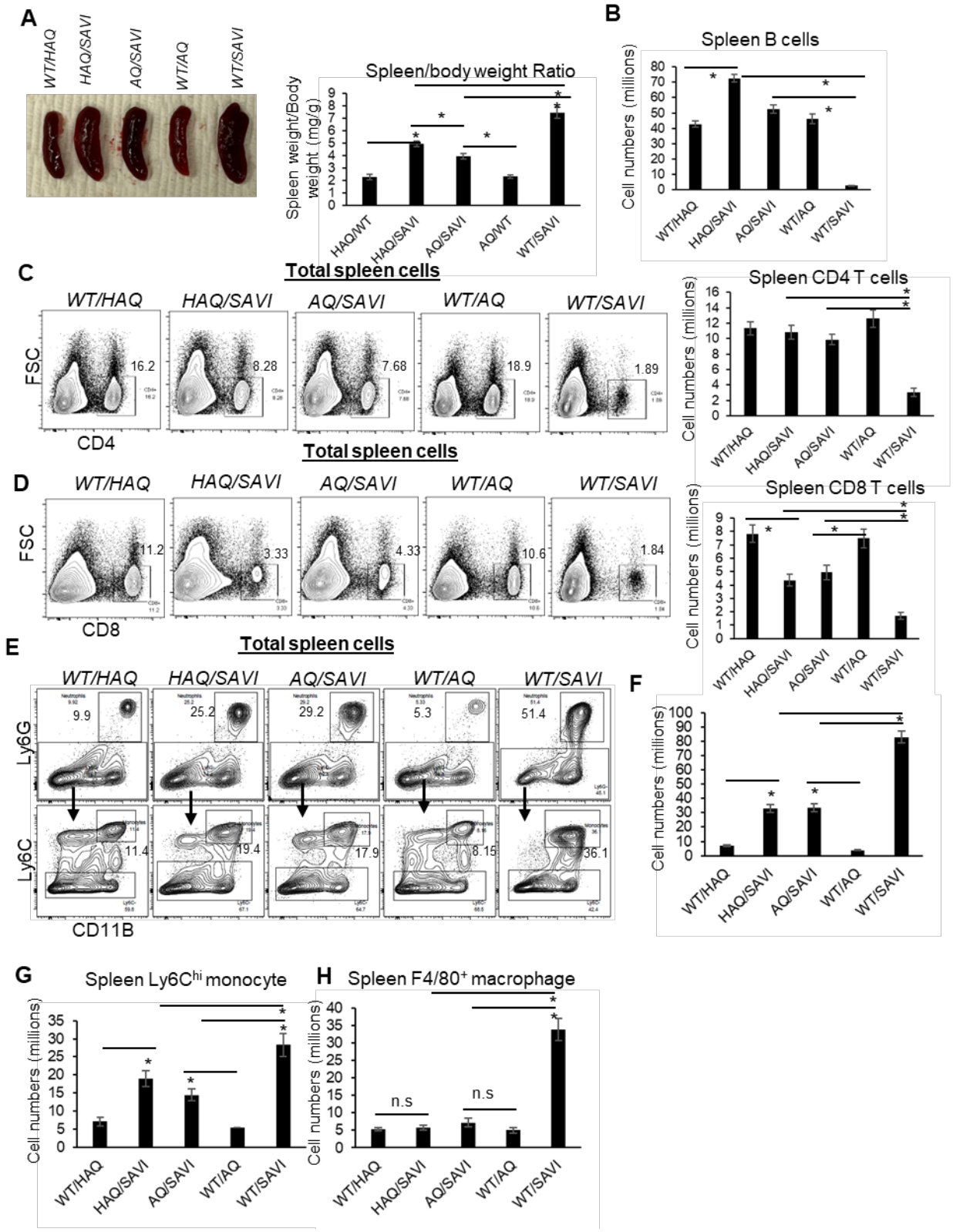

652

653 **Figure 3. *HAQ* and *AQ* rescue the lymphopenia and suppress myeloid cell expansion in *SAVI***

654 ***(N153S)*** **mice. A.** The size and weight of spleens from WT/HAQ, HAQ/SAVI, AQ/SAVI,
655 WT/AQ, WT/SAVI. **B-D.** Spleen $CD19^+$ B cells, CD4, CD8 T cells were determined in the
656 indicated mice by Flow. **E-H.** Spleen $Ly6G^+$ neutrophils, $Ly6C^{hi}$ monocytes and $F4/80^+$
657 macrophage were determined in the indicated mice by Flow. Data are representative of three
658 independent experiments. n=3~5 mice/group. Graphs represent the mean with error bars indication
659 s.e.m. *P* values are determined by one-way ANOVA Tukey's multiple comparison test. * $p<0.05$,
660 n.s: not significant.
661

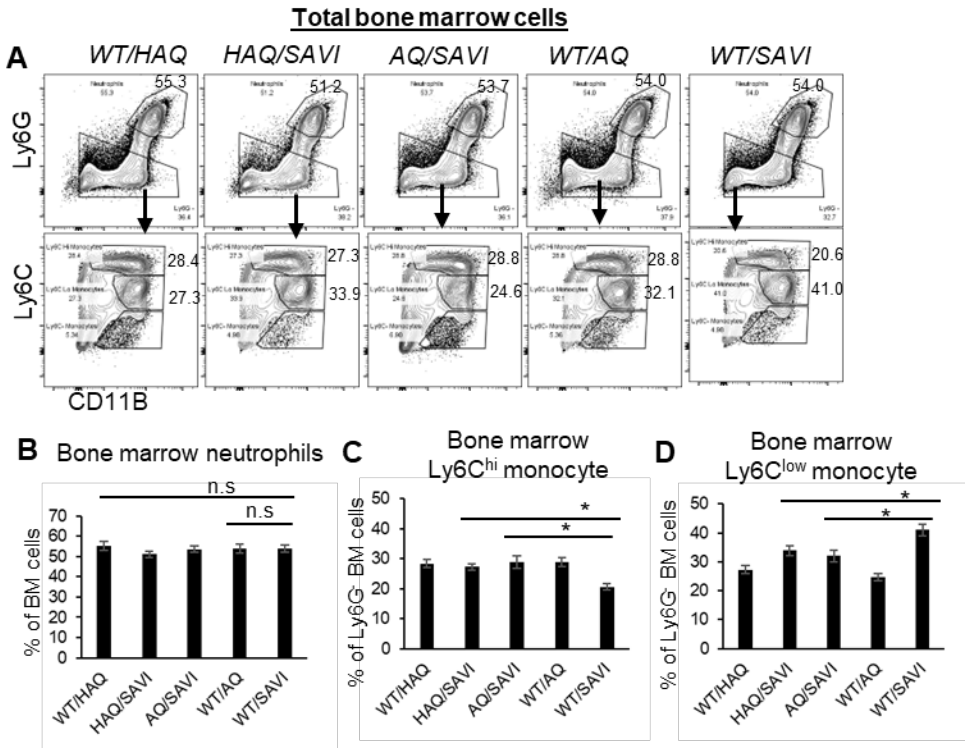

Figure S3. *HAQ* and *AQ* restore bone marrow monocytes in *SAVI (N153S)* mice. A-D. Flow analysis of $Ly6G^{+}CD11B^{+}$ neutrophils and $Ly6G^{-}Ly6C^{+}CD11B^{+}$ bone marrow monocytes from HAQ/SAVI, AQ/SAVI, WT/SAVI and their littermates. n=3~5 mice/group. Data are representative of three independent experiments. Graphs represent the mean with error bars indication s.e.m. *P* values are determined by one-way ANOVA Tukey's multiple comparison test. * $p<0.05$, n.s: not significant.

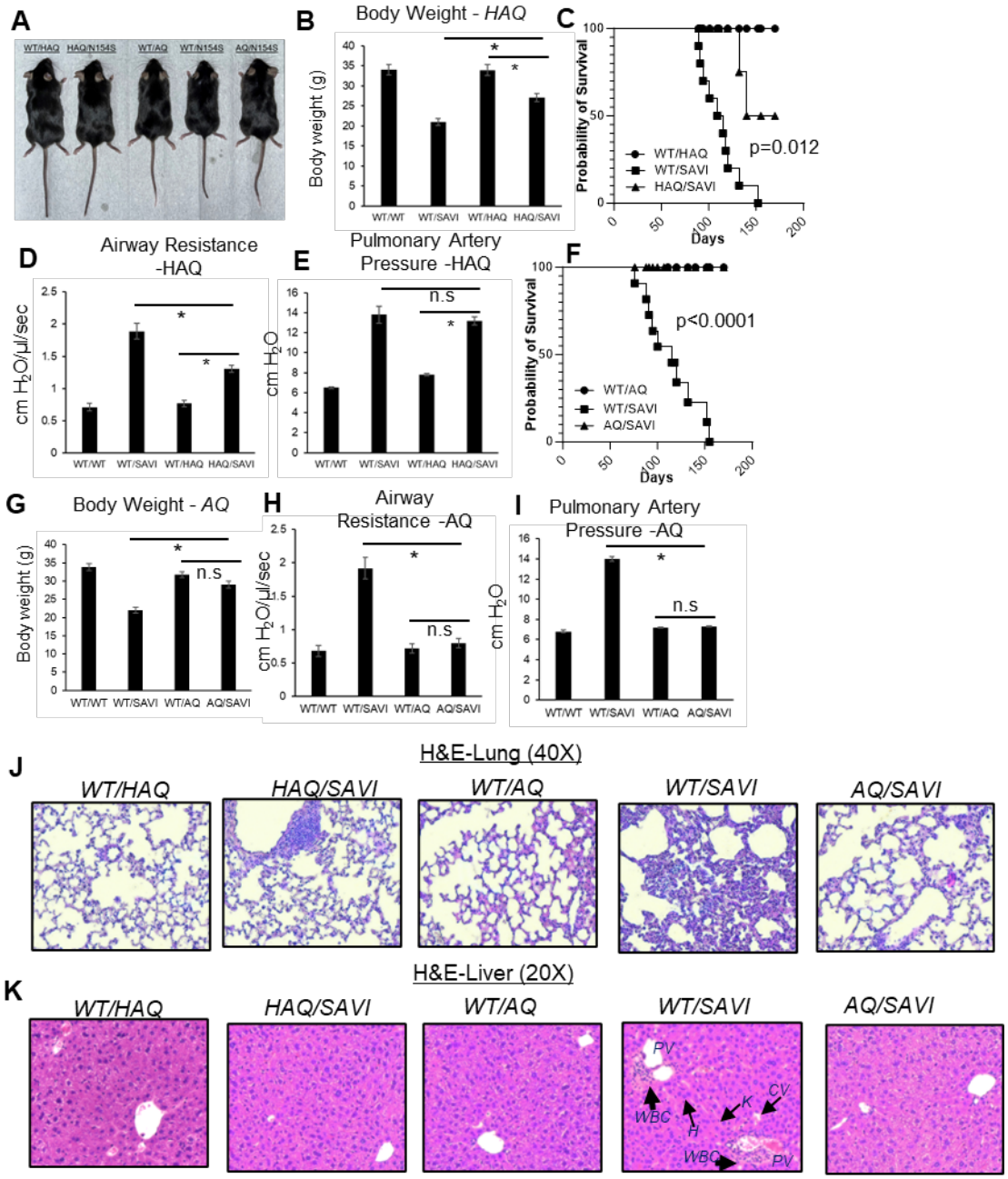

Figure 4. *HAQ* and *AQ* alleles prevent *SAVI(N153S)* disease in mice. A, B, G. The size and body weight of *HAQ/SAVI, AQ/SAVI*, *WT/SAVI* and their littermates *WT/HAQ*, *WT/AQ* mice. **D, E, H, I**. Airway resistance, and pulmonary artery pressure were determined as described in **Materials and Methods**. **C, F.** *HAQ/SAVI, AQ/SAVI, WT/SAVI* (10 mice/group), were monitored for survival by Kaplan-Meier. **J, K.** Representative hematoxylin and eosin (H&E) staining of lung,

676 liver sections from indicated mice. n=3~5 mice/group. Data are representative of at least 2
677 independent experiments. Graphs represent the mean with error bars indication s.e.m. *P* values are
678 determined by one-way ANOVA Tukey's multiple comparison test. * $p<0.05$, ** $p<0.01$. n.s.: not
679 significant. WBC: white blood cells; H: hepatocytes; K: Kupper cells; PV: portal vein; CV: central
680 vein.
681

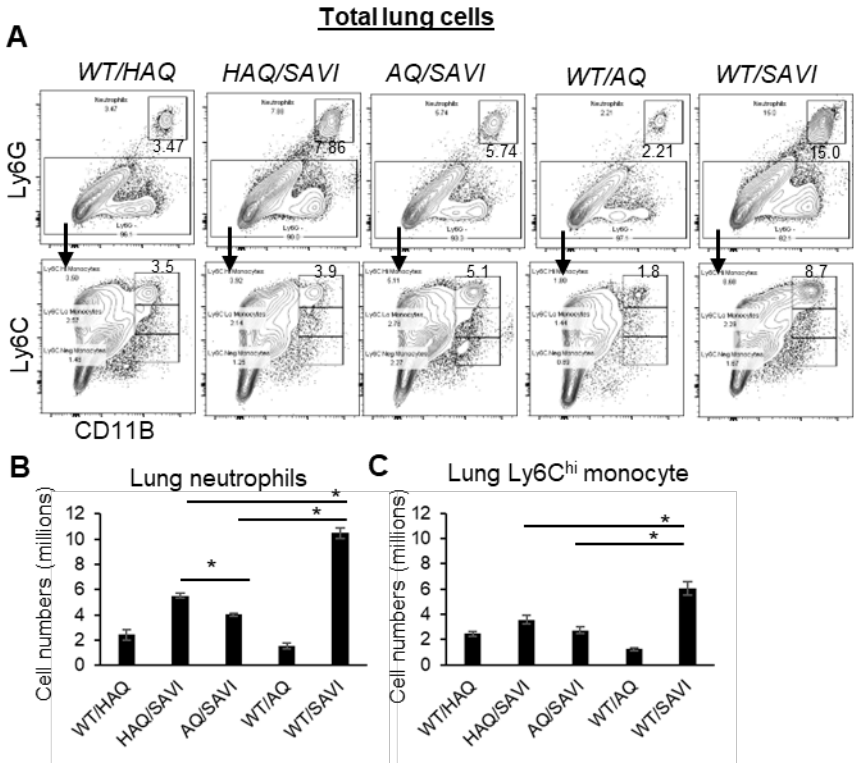

682

683 **Figure S4. *HAQ, AQ* suppress lung myeloid cells infiltration in *SAVI(N153S)* mice**. **A-B.** Flow
684 analysis of lung $Ly6G^{+}CD11B^{+}$ neutrophils and $Ly6G^{-}Ly6C^{+}CD11B^{+}$ monocytes from
685 *HAQ/SAVI, AQ/SAVI, WT/SAVI and their littermates WT/HAQ, WT/AQ* mice. n=3~5 mice/group.
686 Data are representative of three independent experiments. Graphs represent the mean with error
687 bars indication s.e.m. *P* values are determined by one-way ANOVA Tukey's multiple comparison
688 test. * $p<0.05$.

689

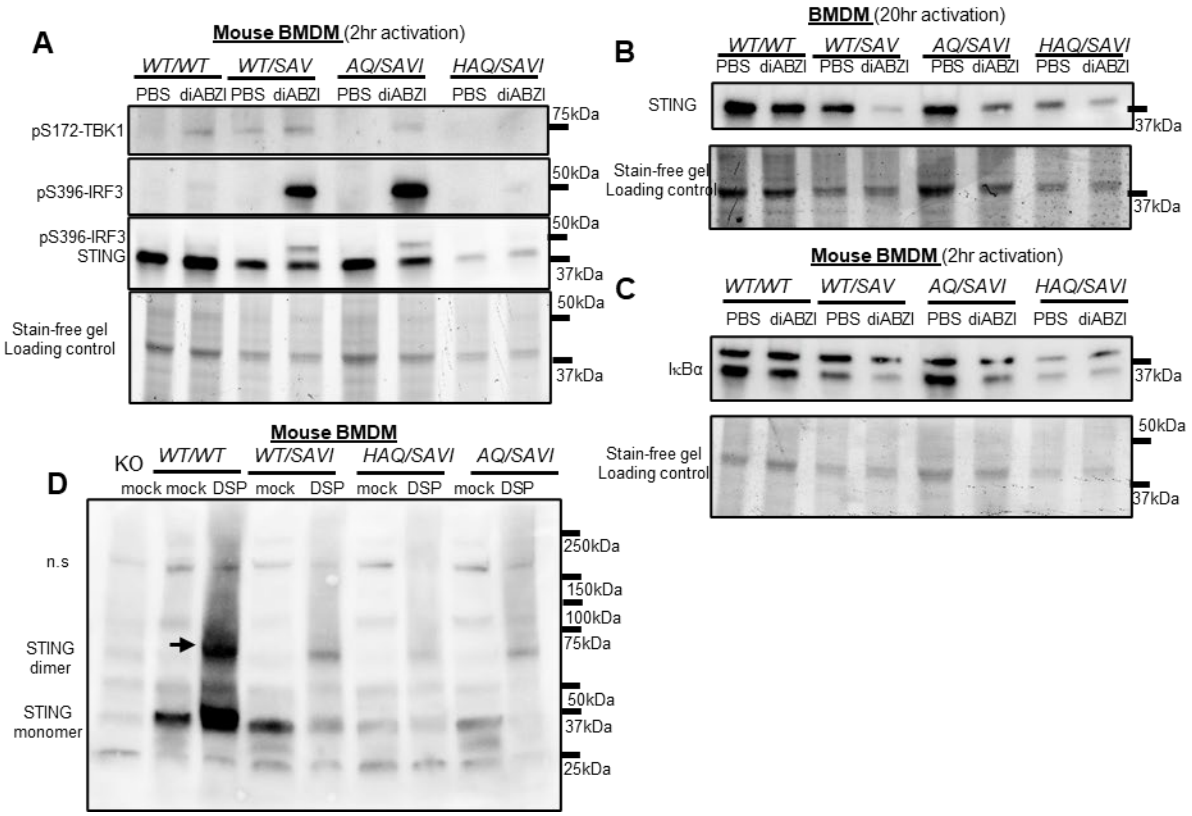

690

691 **Figure 5. *AQ/SAVI(N153S)* cells had similar TBK1-IRF3, NFκB activation and STING**
692 **degradation as the *WT/SAVI(N153S)* cells. A-C.** BMDM from *WT/WT, WT/SAVI, HAQ/SAVI*
693 and *AQ/SAVI* were treated with 100ng/ml diABZi in culture for 2 hrs. Cells were lysed and run on
694 a 4~20% Mini-PROTEAN TGX Stain-Free Precast Gel. The blot was probed for phospho-Thr172-
695 TBK1 antibody (CST, clone D52C2), phosphor-Ser 396-IRF3 (CST, clone 4D4G), STING
696 (Proteintech, #19851-1-AP) and IκBα (CST, clone 44D4) antibody. **B.** BMDM from *WT/WT,*
697 *WT/SAVI, HAQ/SAVI* and *AQ/SAVI* were treated with 100ng/ml diABZi in culture for 24 hrs. Cells
698 were lysed and run on a 4~20% Mini-PROTEAN TGX Stain-Free Precast Gel. The blot was
699 probed for STING antibody (Proteintech, 19851-1-AP). **D.** BMDM from *WT/WT, WT/SAVI,*
700 *HAQ/SAVI* and *AQ/SAVI* were treated with 400μM cleavable chemical crosslinker DSP (Pierce™,
701 cat no: PG82081) in PBS for 1 hr at 4°C. Cells were washed with PBS and lysed in RIPA buffer.
702 Whole cell lysate was mixed with 4x Laemmli Sample Buffer (BioRad, cat no 1610747) containing

703 5% 2-mercaptoethanol, heated at 95°C for 10 min and, run on a 4~20% Mini-PROTEAN TGX
704 Stain-Free Precast Gel. The blot was probed for STING antibody (Proteintech, 19851-1-AP). Data
705 are representative of three independent experiments.
706

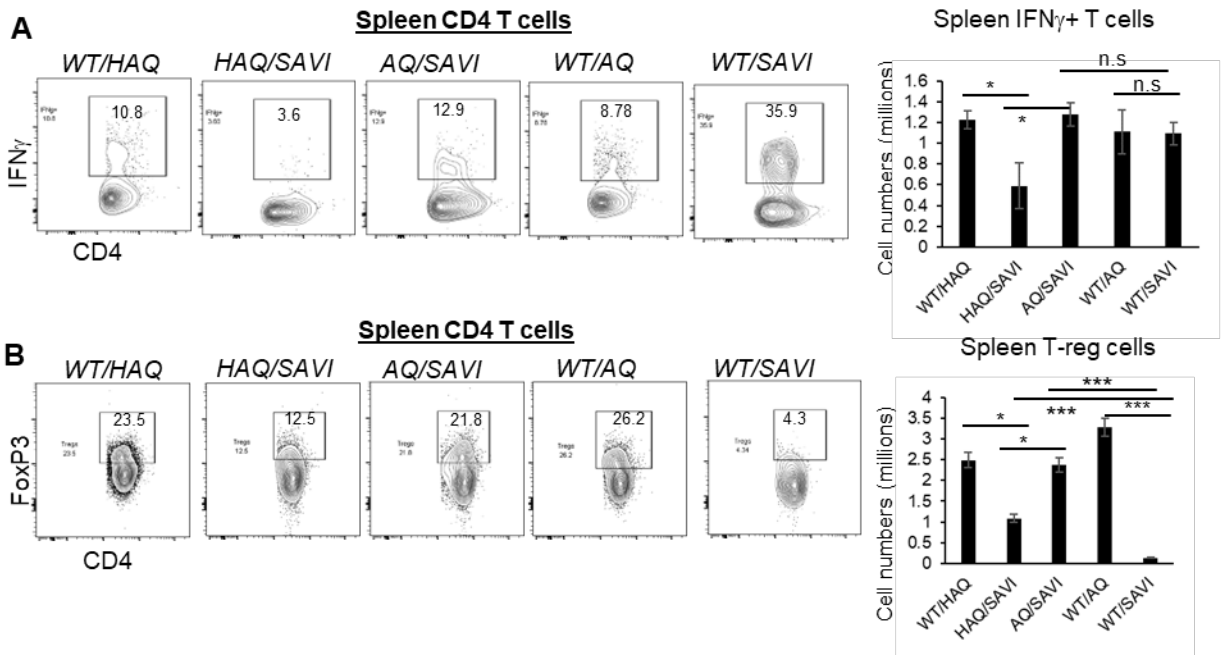

707

708 **Figure 6. *HAQ/SAVI(N153S)* and *AQ/SAVI(N153S)* cells had 10-fold and 20-fold increased**
709 **spleen T-regs compared to *WT/SAVI* mice. A.** Flow cytometry analysis of IFNγ producing
710 spleen $CD4^+$ T cells from *WT/HAQ, WT/AQ, WT/SAVI, HAQ/SAVI* and *AQ/SAVI* mice. **B**. Flow
711 cytometry analysis of $CD4^+$ $FoxP3^+$ spleen T-regs. n=3~5 mice/group. Data are representative of
712 at least 2 independent experiments. Graphs represent the mean with error bars indication s.e.m. *P*
713 values are determined by one-way ANOVA Tukey's multiple comparison test. * $p<0.05$,
714 ** $p<0.01$, *** $p<0.001$. n.s.: not significant.